

Reactivity and Mechanism of Stable Heterocyclic Silylenes with Carbon Tetrachloride

Ruei-En Li, Jeng-Horng Sheu, and Ming-Der Su*

Department of Applied Chemistry, National Chiayi University, Chiayi 60004, Taiwan

Received June 25, 2007

The potential energy surfaces for the reactions of stable silylenes with carbon tetrachloride have been characterized in detail using density functional theory [B3LYP/6-311G(d)], including zero-point corrections. Five stable silylene species (1–5) have been chosen in this work as model reactants. The activation barriers and enthalpies of the reactions are compared to determine the relative reactivity of the stable silylenes on the reaction potential energy surface. Our theoretical findings suggest that stable silylene **5**, which has two carbon atoms bonded to the silicon center and does not contain a resonance structure, is relatively unstable with respect to the reaction with haloalkanes, in comparison with the other stable silylenes (1–4). Of the three possible reaction paths, Cl abstraction (path 1), CCl₃ abstraction (path 2), and CCl₄ insertion (path 3), path 1 is found to be most favorable, with a very low activation energy and a large exothermicity. In short, electronic as well as steric factors play a dominant role in determining the chemical reactivity of the stable silylene species kinetically as well as thermodynamically. Furthermore, a configuration mixing model based on the work of Pross and Shaik is used to rationalize the computational results. The results obtained allow a number of predictions to be made.

I. Introduction

Over the past decade, silylene chemistry has received serious attention.¹ One reason for this activity is an interest in understanding how silylenes play a key role in many thermal and photochemical reactions of organosilicon compounds.² Nevertheless, it seems to be generally accepted that silylenes cannot be stabilized at room temperature.³ In fact, many silylenes, which have been observed and identified when isolated in argon or hydrocarbon matrices at very low temperatures, are extremely unstable, decomposing rapidly at temperatures above 77 K.³ It was not until 1994 that the first thermally stable silylene, **1**, was synthesized and isolated.^{3,4} Since then, several stable silylenes have been reported, including **2**,⁴ **3**,⁵ **4**,⁶ and **5**.⁷ It has been suggested

that, although the *tert*-butyl groups provide some kinetic and steric stabilization to these silylenes, electronic factors arising from the pseudoaromaticity of the species or π donation from nitrogen to silicon are primarily responsible for the stability of these systems.^{1,4} In principle, the availability of stable silylenes has allowed the discovery of new compounds and

* To whom correspondence should be addressed. E-mail: midesu@mail.ncyu.edu.tw.

(1) For the most recent reviews, see: (a) Gaspar, P. P.; West, R. In *The Chemistry of Organic Silicon Compounds*, 2nd ed.; Rappoport, Z., Apeloig, Y., Eds.; Wiley: New York, 1999; Part 3, pp 2463–2568. (b) Haaf, M.; Schmedake, T. A.; West, R. *Acc. Chem. Res.* **2000**, *33*, 704. (c) Gehrhus, B.; Lappert, M. F. *J. Organomet. Chem.* **2001**, *607*–608, 209. (d) Hill, N. J.; West, R. *J. Organomet. Chem.* **2004**, *689*, 4165. (e) Kira, M. *J. Organomet. Chem.* **2004**, *689*, 4475. (f) Kuhl, O. *Coord. Chem. Rev.* **2004**, *248*, 411. (g) Alder, R. W.; Blake, M. E.; Chaker, L.; Harvey, J. N.; Paolini, F.; Schutz, J. *Angew. Chem., Int. Ed.* **2004**, *43*, 5896. (h) Gehrhus, B.; Hitchcock, P. B.; Pongtavorpinyo, R.; Zhang, L. *J. Chem. Soc., Dalton Trans.* **2006**, *15*, 1847.

(2) For instance, see: (a) Okazaki, R.; Tokitoh, N. *Acc. Chem. Res.* **2000**, *33*, 625. (b) Tokitoh, N.; Matsumoto, T.; Okazaki, R. *Bull. Chem. Soc. Jpn.* **1999**, *72*, 1665. (c) Auner, N.; Weis, J. *Organosilicon Chemistry*; VCH: Weinheim, Germany, 1994. (d) Auner, N.; Weis, J. *Organosilicon Chemistry II*; VCH: Weinheim, Germany, 1996. (e) Auner, N.; Weis, J. *Organosilicon Chemistry III*; VCH: Weinheim, Germany, 1998. (f) Auner, N.; Weis, J. *Organosilicon Chemistry IV*; VCH: Weinheim, Germany, 2000. (g) Gaspar, P. P. In *Reactive Intermediates*; Jones, M., Jr., Moss, R. A., Eds.; Wiley: New York, 1981; Vol. 2, pp 335–385. (h) Gaspar, P. P. In *Reactive Intermediates*; Jones, M., Jr., Moss, R. A., Eds.; Wiley: New York, 1985; Vol. 3, pp 333–427. (i) Jasinski, J. M.; Meyerson, B. S.; Scott, B. A. *Annu. Rev. Phys. Chem.* **1987**, *38*, 109.

(3) Denk, M.; Lennon, R.; Hayashi, R.; West, R.; Haaland, A.; Belyakov, H.; Verne, P.; Wagner, M.; Metzler, N. *J. Am. Chem. Soc.* **1994**, *116*, 2691.

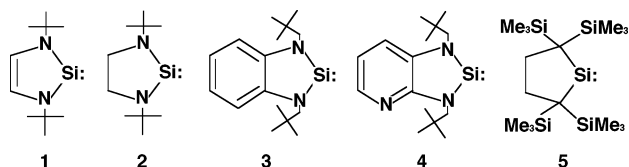
(4) (a) West, R.; Denk, M. *Pure Appl. Chem.* **1996**, *68*, 785. (b) Haaf, M.; Schmedake, T. A.; Paraduse, B. J.; West, R. *Can. J. Chem.* **2000**, *78*, 1526.

(5) Gehrhus, B.; Lappert, M. F.; Heinicke, J.; Boose, R.; Balaser, D. *J. Chem. Soc., Chem. Commun.* **1995**, 1931.

(6) Heinicke, J.; Oprea, A.; Kindermann, M. K.; Karpati, T.; Byulaszi, L.; Veszpremi, T. *Chem.—Eur. J.* **1998**, *4*, 541.

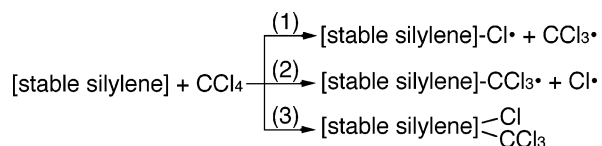
(7) Kira, M.; Ishida, S.; Iwamoto, T.; Kabuto, C. *J. Am. Chem. Soc.* **1999**, *121*, 9722.

Scheme 1



novel reaction chemistry.⁸ However, little is known about the behavior of silylenes toward haloalkanes. Indeed, to the best of our knowledge, until now neither experimental nor theoretical work has been devoted to detailed mechanistic studies of the reactions of stable silylenes with haloalkanes, let alone a systematic study of the effects of the reactivities of a series of stable silylene species such as the shown in Scheme 1.⁹

This has prompted us to investigate the reactions of stable silylenes with haloalkanes. A detailed understanding of stable silylene reactivity is of interest not only for the advancement of basic science but also for the continued development of their applications. We therefore present a density functional theory (DFT) study of the following reactions ([stable silylene] stands for the stable silylenes **1–5** given in Scheme 1):



That is, three competitive reaction pathways have been proposed for the initial reactions of stable silylenes with carbon tetrachloride. Basically, two are radical pathways proceeding either via a chlorine atom, **Cl-Abs** (path 1), or via a CCl_3 group abstraction, **CCl_3 -Abs** (path 2). The third possible pathway is an insertion in which the central silicon atom of the stable silylene inserts into a C–Cl bond of carbon tetrachloride, **Ins** (path 3). The reason for choosing CCl_4 is only because experiments on this compound were available for comparison.¹⁰

The aims of this work are threefold: (I) to determine which reaction pathway predominates and to provide essential information about the mechanism of the reaction; (II) to obtain a detailed understanding of the energetics and kinetics of the transfer of either a chlorine atom or a CCl_3 group from CCl_4 to a stable silylene, as well as those for the insertion reaction with CCl_4 ; (III) to probe the dominant factors affecting the reactivities of these stable silylenes. From these investigations, it is hoped that, in view of recent dramatic developments in stable silylene chemistry, analogous extensive studies of their reactions with haloalkanes should soon be forthcoming and will open up new areas.

- (8) For instance, see: (a) West, R.; Schmedake, T. A.; Haaf, M.; Becker, J.; Mueller, T. *Chem. Lett.* **2001**, 68. (b) Lee, M. E.; Cho, H. M.; Kim, C. H.; Ando, W. *Organometallics* **2001**, 20, 1472. (c) Avent, A. G.; Gehrhus, B.; Hitchcock, P. B.; Lappert, M. F.; Maciejewski, H. *J. Organomet. Chem.* **2003**, 686, 321. (d) Naka, A.; Hill, N. J.; West, R. *Organometallics* **2003**, 23, 6330. (e) Moser, D.; Naka, A.; Guzei, I. A.; Muller, T.; West, R. *J. Am. Chem. Soc.* **2005**, 116, 2691. (9) Li, W.; Hill, N. J.; Tomasiak, A. C.; Bikzhanova, G.; West, R. *Organometallics* **2006**, 25, 3802.

II. Theoretical Methods

All geometries were fully optimized without imposing any symmetry constraints, although in some instances the resulting structure showed various elements of symmetry. For our DFT calculations, we used the hybrid gradient-corrected exchange functional proposed by Becke,¹¹ combined with the gradient-corrected correlation functional of Lee, Yang, and Parr.¹² This functional is commonly known as B3LYP and has been shown to be quite reliable for both geometries and energies.¹³ The geometries and energetics of the stationary points on the potential energy surface were calculated using the DFT (B3LYP) method in conjunction with the 6-311G(d) basis set.¹⁴ We denote our B3LYP calculations by B3LYP/6-311G(d). The spin-unrestricted (UB3LYP) formalism was used for the open-shell (doublet) species. The S^2 expectation values of the doublet and triplet states for the calculated species all showed ideal values (2.00 and 0.75, respectively) after spin annihilation, so that their geometries and energetics are reliable for this study. Frequency calculations were performed on all structures to confirm that the reactants, intermediates, and products had no imaginary frequencies and that transition states possessed only one imaginary frequency. The relative energies were corrected for vibrational zero-point energies (not scaled). All of the DFT calculations were performed using the *GAUSSIAN 03* package of programs.¹⁵

III. Results and Discussion

(1) Geometries and Energetics of Stable Silylenes.

Before discussing the geometrical optimizations and the potential energy surfaces for the reactions, we first review the geometries of the reactants, i.e., the stable silylenes **1–5**. It should be mentioned that, for the sake of simplicity, we have used CH_3 substituent groups, instead of CMe_3 groups, in several stable dialkylsilylene molecules (such as **1–4**). Also, we have used SiH_3 substituent groups, instead of SiMe_3 groups, in the stable silylene molecule (**5**). Our calculated geometrical parameters for the closed-shell species, based on the B3LYP/6-311G(d) level of theory, are collected in Figure 1, where they are compared with some available experimental values given in parentheses.^{3–5,7}

- (10) Su, M. D. *Inorg. Chem.* **2004**, 43, 4846.
 (11) (a) Becke, A. D. *Phys. Rev. A* **1988**, 38, 3098. (b) Becke, A. D. *J. Chem. Phys.* **1993**, 98, 5648.
 (12) Lee, C.; Yang, W.; Parr, R. G., *Phys. Rev. B* **1988**, 37, 785.
 (13) (a) Su, M. D. *J. Phys. Chem. A* **2004**, 108, 823. (b) Su, M.-D. *Inorg. Chem.* **2004**, 43, 4846. (c) Su, M. D. *Chem.—Eur. J.* **2005**, 10, 5877.
 (14) (a) Dunning, T. H., Jr.; Hay, P. J. In *Modern Theoretical Chemistry*; Schaefer, H. F., III, Ed.; Plenum: New York, 1976; pp 1–28.
 (15) Frisch, M. J.; Trucks, G. W.; Schlegel, H. B.; Scuseria, G. E.; Robb, M. A.; Cheeseman, J. R.; Zakrzewski, V. G.; Montgomery, J. A., Jr.; Vreven, T.; Kudin, K. N.; Burant, J. C.; Millam, J. M.; Iyengar, S. S.; Tomasi, J.; Barone, V.; Mennucci, B.; Cossi, M.; Scalmani, G.; Rega, N.; Petersson, G. A.; Nakatsuji, H.; Hada, M.; Ehara, M.; Toyota, K.; Fukuda, R.; Hasegawa, J.; Ishida, M.; Nakajima, T.; Honda, Y.; Kitao, O.; Nakai, H.; Klene, M.; Li, X.; Knox, J. E.; Hratchian, H. P.; Cross, J. B.; Adamo, C.; Jaramillo, J.; Gomperts, R.; Stratmann, R. E.; Yazyev, O.; Austin, A. J.; Cammi, R.; Pomelli, C.; Ochterski, J. W.; Ayala, P. Y.; Morokuma, K.; Voth, G. A.; Salvador, P.; Dannenberg, J. J.; Zakrzewski, V. G.; Dapprich, S.; Daniels, A. D.; Strain, M. C.; Farkas, O.; Malick, D. K.; Rabuck, A. D.; Raghavachari, K.; Foresman, J. B.; Ortiz, J. V.; Cui, Q.; Baboul, A. G.; Clifford, S.; Cioslowski, J.; Stefanov, B. B.; Liu, G.; Liashenko, A.; Piskorz, P.; Komaromi, I.; Martin, R. L.; Fox, D. J.; Keith, T.; Al-Laham, M. A.; Peng, C. Y.; Nanayakkara, A.; Challacombe, M.; Gill, P. M. W.; Johnson, B.; Chen, W.; Wong, M. W.; Gonzalez, C.; Pople, J. A. *GAUSSIAN 03*; Gaussian, Inc.: Wallingford, CT, 2003.

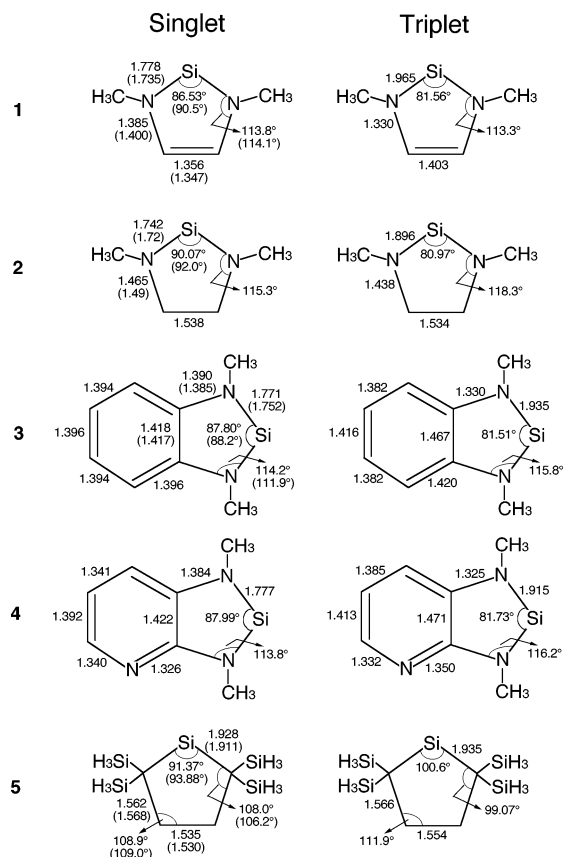


Figure 1. Optimized geometrical parameters of stable silylenes **1–3** and **5** based on the B3LYP/6-311G(d) method, compared with the available experimental data (in parentheses). See refs 3–5 and 7, respectively.

Although only a few details concerning their geometrical parameters are as yet available, we can compare some of our results with those obtained for stable silylenes. As one can see in Figure 1, the molecular parameters for our B3LYP/6-311G(d) calculations agree reasonably well with the experimental data,^{3–5,7} bearing in mind that the synthesized molecules contain bulkier substituents. For example, our calculated Si–N bond lengths in **1** (1.778 Å), in **2** (1.742 Å), in **3** (1.771 Å), and in **5** (1.928 Å) compare favorably with those determined from X-ray data in **1** (1.735 Å) synthesized by Denk et al.,³ **2** (1.72 Å) prepared by Denk et al.,⁴ **3** (1.752 Å) reported by Lappert et al.,⁵ and **5** (1.911 Å) identified by Kira et al.,⁷ respectively. In these stable silylene molecules, the valence angles at the silicon center (90.5°, 92.0°, 88.2°, and 93.88°) are somewhat wider than those calculated for our closed-shell species (86.53°, 90.07°, 87.80°, and 91.37° at the B3LYP level, respectively). This may be attributed to the larger size of the alkyl substituents at the nitrogen centers that cause substituted stable silylenes to have larger bond angles than the parent stable silylene itself. In any event, the good agreement between our computational results and available experimental data is quite encouraging. We therefore believe that the B3LYP/6-311G(d) level employed in this work can provide reasonable molecular geometries as well as energetics for those chemical reactions for which experimental data are still not available.

Furthermore, as one can see in Figure 1, in the case of stable silylene reactants (**1–4**), the triplet state has a

Table 1. Relative Energies (All in kcal/mol) for Singlet and Triplet Stable Silylenes and for the Process Stable Silylenes (**1–5**) + CCl₄ → Transition State → Products^{a,b}

system	ΔE_{st}^c	path 1		path 2		path 3	
		$\Delta E^\ddagger d$	ΔH^e	$\Delta E^\ddagger d$	ΔH^e	$\Delta E^\ddagger d$	ΔH^e
1	+53.32	+8.868	+4.822	+52.48	+35.65	+31.42	–51.31
2	+68.02	+8.830	+5.685	+53.06	+37.44	+28.21	–62.80
3	+59.56	+8.117	+7.229	+55.87	+38.63	+30.88	–55.05
4	+58.99	+9.784	+7.534	+57.03	+38.98	+30.36	–55.41
5	+33.56	+3.572	–12.28	+47.36	+23.74	+13.35	–72.34

^a At the B3LYP/6-311G(d) level of theory. For the B3LYP-optimized structures of the stationary points, see Figures 2–6. ^b Energy differences have been zero-point-corrected. See the text. ^c Energy relative to the corresponding singlet state. A positive value means the singlet is the ground state. ^d The activation energy of the transition state, relative to the corresponding reactants. ^e The reaction enthalpy of the product, relative to the corresponding reactants.

significantly longer bond distance (Si–N) and narrower bond angle (\angle NSiN) than the corresponding closed-shell singlet state. The reason for this phenomenon can be understood simply by considering their electronic structures.¹⁵ See Figure 2. As discussed previously,¹⁶ the highest occupied molecular orbital (HOMO) and lowest unoccupied molecular orbital (LUMO) for a cyclic silylene are π_3 and π_5 orbitals, respectively. As a result, in the triplet state of stable silylenes (**1–4**), one electron is situated in the π_5 orbital, in which there are antibonding interactions between the silicon center and nitrogen and carbon atoms. This orbital is empty in the singlet state. The additional occupation of π_5 therefore leads to a weakening of the Si–N bonds and a narrowing of the \angle NSiN angle. This qualitative argument agrees with our computational results obtained at the B3LYP level of theory as given in Figure 1.

However, as seen in Figure 1, the triplet state of stable silylene **5** has a significantly wider bond angle (\angle CSiC) and longer bond distance (Si–C) than its closed-shell singlet state. Again, the reason for this phenomenon can be understood simply by considering its electronic structure. In contrast to the case of a simple silylene,¹⁷ the HOMO of stable silylene **5** is essentially a nonbonding σ orbital. This lone-pair orbital is arranged in the cyclic plane, in a pseudotrigonal planar fashion with respect to the two sets of Si–C linkages. As a result, such a lone pair can be viewed as located within an orbital of predominant sp character. On the other hand, our computational results show that the LUMO of stable silylene **5** corresponds to the silicon vacant p– π orbital. Accordingly, the dominant configuration of a singlet stable silylene **5** is $\sigma^2\pi^0$, while that of a triplet is $\sigma^1\pi^1$. As a result, the optimum Si–C bond lengths in the triplet are longer than those in the singlet state. This is presumably due to the fact that conjugation of the triplet silylene π electron with the two π electrons of the π -donor group is less important than the delocalization of the latter into the empty p– π orbital on the stable silylene silicon atom in the singlet state. This, in turn, would make the bond angle (\angle CSiC) in the triplet state larger than that in closed-shell

(16) Su, M. D.; Chu, S. Y. *Inorg. Chem.* **1999**, *38*, 4819.

(17) Herrmann, W.; Kocher, C. *Angew. Chem., Int. Ed. Engl.* **1997**, *36*, 2163 and references cited therein.

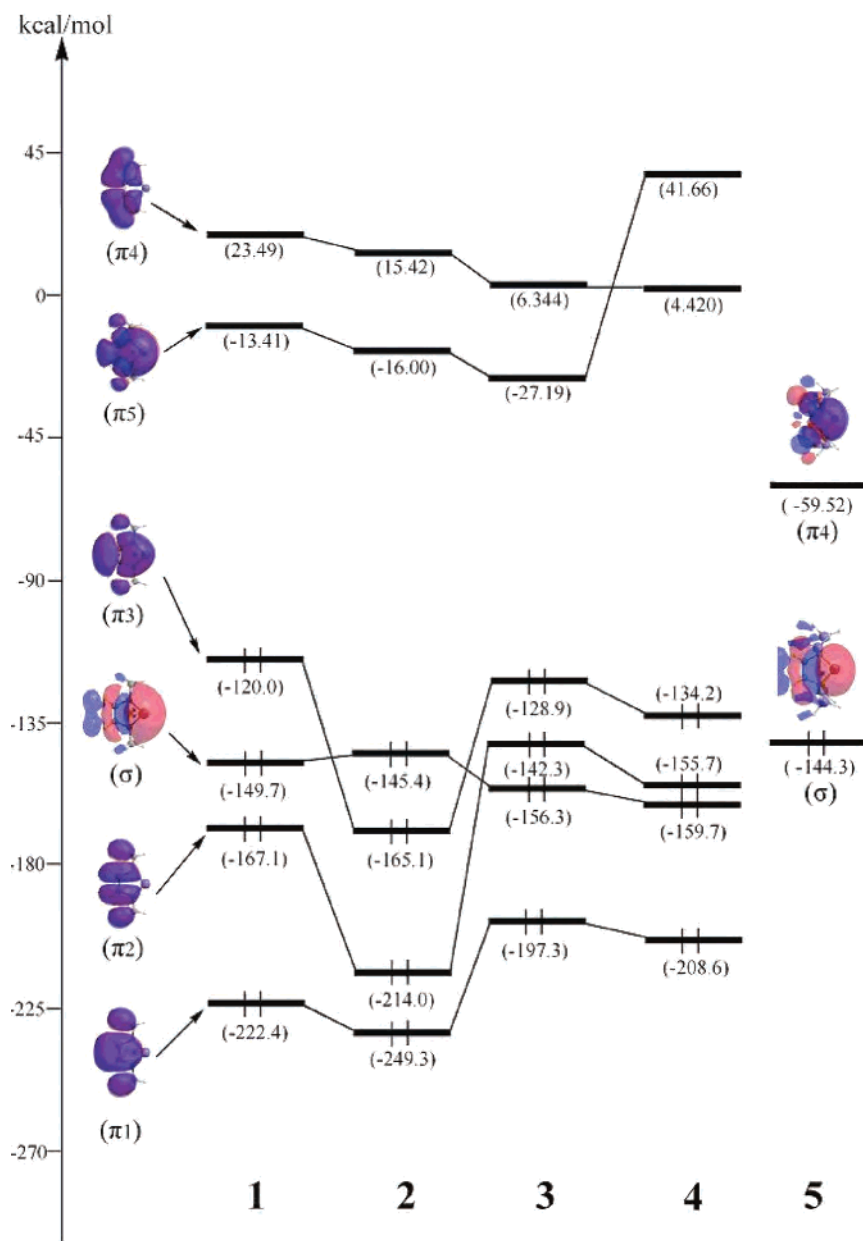


Figure 2. Schematic representation of the relative energies (au) for frontier orbitals of stable cyclic silylenes (1–5) based on the B3LYP/6-311G(d) calculations, compared with the stable cyclic carbene. For more information, see the text.

singlet state. These predictions based on the electronic structures are consistent with the computational results presented in this work.

Calculated values for the energy difference ΔE_{st} ($=E_{\text{triplet}} - E_{\text{singlet}}$) between the singlet and triplet states of various stable silylenes (1–5) are given in Table 1; a positive value for ΔE_{st} implies that the singlet is predicted to be the ground state rather than the triplet state. According to Table 1, our calculations indicate that all of the above stable silylene species (1–5) should have a singlet ground state. Moreover, our B3LYP results indicate that the singlet–triplet splittings for these stable silylenes are 53.3 (1), 68.0 (2), 59.6 (3), 59.0 (4), and 33.6 (5) kcal/mol, respectively; i.e., ΔE_{st} decreases in the order $2 > 3 > 4 > 1 > 5$. We use the above results to explain the origin of barrier heights for chemical reactions in a later section.

Finally, it should be noted that for all of the silylenes studied in this work the excitation energies from the singlet ground state to the first triplet excited state are quite large (ca. 34–68 kcal/mol). This means that thermal production of the first excited triplet state under experimental conditions is practically impossible. Thus, only the singlet potential surface has been considered throughout this work.

(2) Transition States for Abstraction Reactions. As mentioned in the Introduction, the initial reaction of a stable silylene with carbon tetrachloride can take place from three directions: via abstraction of a chlorine atom from CCl_4 to produce (stable silylene) Cl^\bullet and CCl_3^\bullet (**Cl-Abs**; path 1), via CCl_3^\bullet radical transfer to stable silylene leading to the formation of (stable silylene) CCl_3^\bullet and Cl^\bullet (**CCl_3 -Abs**; path 2), and finally via an insertion reaction with CCl_4 (**Ins**; path 3). The main geometrical parameters of the transition states

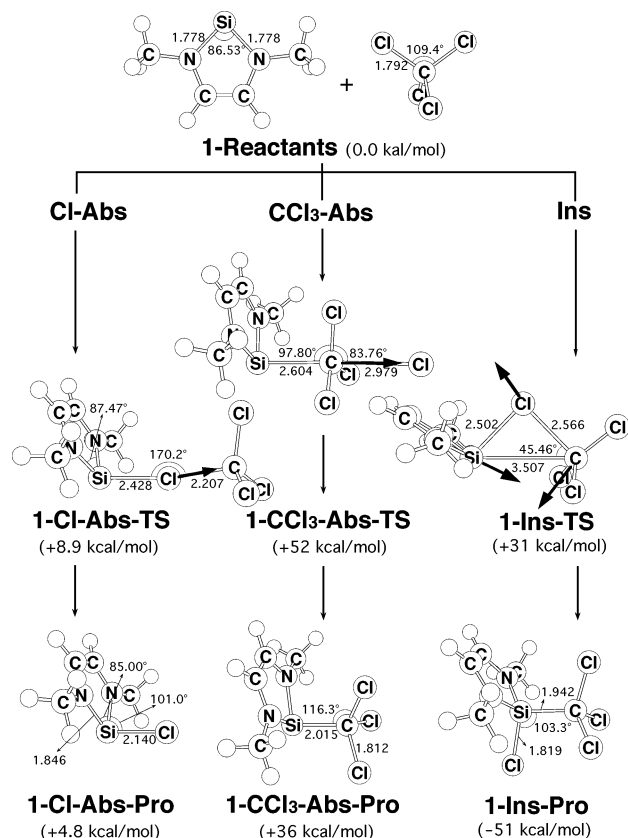


Figure 3. Optimized geometries (in Å and deg) for the reactants, transition states (TSs), and products (Pros) of stable cyclic silylene (**1**) with CCl₄ through three reaction pathways, i.e., the one-Cl abstraction (Cl-Abs), the one-CCl₃-group abstraction (CCl₃-Abs), and the insertion reaction (Ins). All were calculated at the B3LYP/6-311G(d) level of theory. The heavy arrows indicate the main components of the transition vector. Hydrogen atoms are omitted for clarity.

corresponding to the two possible abstraction reactions as well as their appearance are shown in Figures 3–7, together with the meaningful components of their transition vectors. The results for the transition states of the stable silylene abstraction and insertion reactions might perhaps be some of the most interesting results of the present study because neither experiments nor theory has yet studied their barrier heights.

The transition states for the stable silylenes (**1**–**5**) will be referred to as **1-Cl-Abs-TS**, **2-Cl-Abs-TS**, **3-Cl-Abs-TS**, **4-Cl-Abs-TS**, **5-Cl-Abs-TS**, and **1-CCl₃-Abs-TS**, **2-CCl₃-Abs-TS**, **3-CCl₃-Abs-TS**, **4-CCl₃-Abs-TS**, **5-CCl₃-Abs-TS**, and **1-Ins-TS**, **2-Ins-TS**, **3-Ins-TS**, **4-Ins-TS**, **5-Ins-TS** for path 1 (Cl abstraction), path 2 (CCl₃ abstraction), and path 3 (insertion), respectively.

The main component of the transition vector of Cl abstraction corresponds to the motion of the chlorine atom between the silicon and carbon atoms. The eigenvalues give imaginary frequencies of 103*i* (**1-Cl-Abs-TS**), 103*i* (**2-Cl-Abs-TS**), 112*i* (**3-Cl-Abs-TS**), 150*i* (**4-Cl-Abs-TS**), and 121*i* (**5-Cl-Abs-TS**) cm⁻¹. Indeed, inspection of the transition vector shows clearly that the reaction proceeds toward the formation of (stable silylene)Cl[•] and CCl₃[•]. It should be pointed out here that the three atoms (Si, Cl', and C; Cl' = migrating chlorine atom) involved in the bond-breaking and

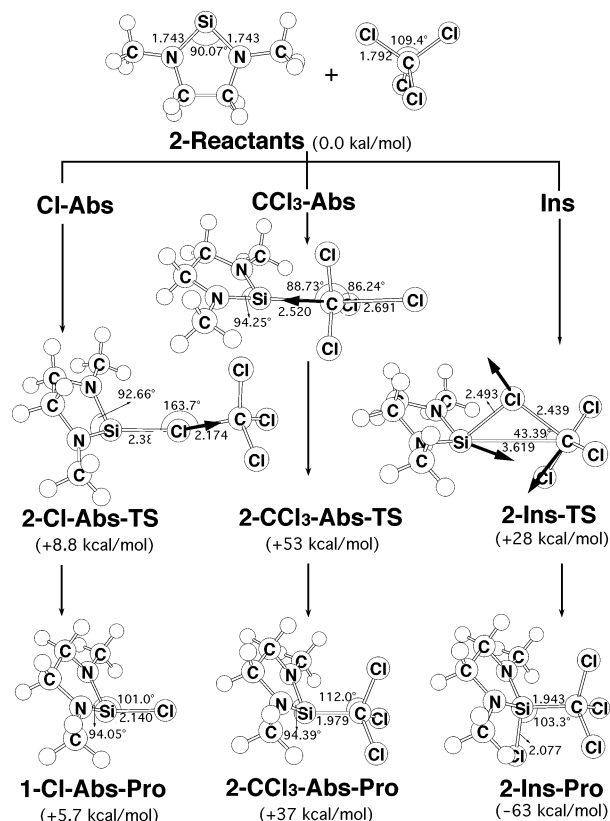


Figure 4. Optimized geometries (in Å and deg) for the reactants, transition states (TSs), and products (Pros) of stable cyclic silylene (**2**) with CCl₄ through three reaction pathways, i.e., the one-Cl abstraction (Cl-Abs), the one-CCl₃-group abstraction (CCl₃-Abs), and the insertion reaction (Ins). All were calculated at the B3LYP/6-311G(d) level of theory. The heavy arrows indicate the main components of the transition vector. Hydrogen atoms are omitted for clarity.

bond-forming processes are not collinear along the Cl'–C axis, as displayed in Figures 3–7. The silicon atom makes an angle, with respect to the Cl'–C bond, of 170°, 164°, 168°, 167°, and 156° for stable silylenes **1**–**5**, respectively. One of the interesting points to emerge from calculations of the transition state geometries is the extent to which the Si–Cl' bond is formed in the transition state. Relative to its value in the product (*vide infra*), the Si–Cl bond lengths in **1-Cl-Abs-TS**, **2-Cl-Abs-TS**, **3-Cl-Abs-TS**, **4-Cl-Abs-TS**, and **5-Cl-Abs-TS** are 13%, 12%, 17%, 14%, and 18%, respectively, longer than those in the corresponding products. In addition, the distances of the Cl'–C bond to be broken are 23%, 21%, 18%, 21%, and 14% longer than that of the corresponding reactant CCl₄. All of this suggests that the stable silylene **5** Cl-abstraction reaction arrives at its transition state relatively early, whereas the stable silylene **2** reaction reaches its transition state relatively late. As a consequence, the barrier is encountered earlier in the abstractions of the former than of the latter. As will be shown below, this is consistent with the Hammond postulate,¹⁸ which associates an earlier transition state with a lower barrier and a more exothermic reaction.

We now consider the CCl₃ abstraction reaction (path 2). A search for the transition state revealed that the energy

(18) Hammond, G. S. *J. Am. Chem. Soc.* **1954**, *77*, 334.

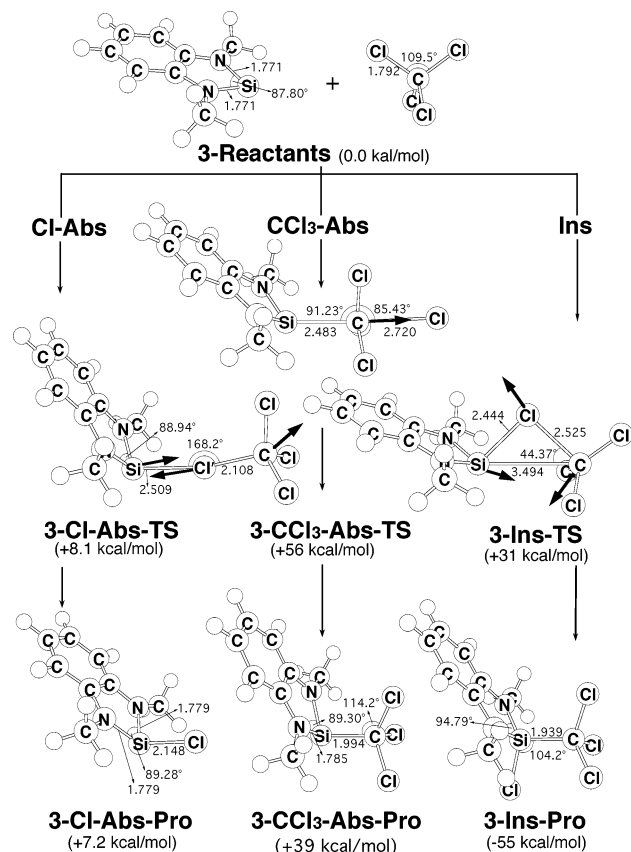


Figure 5. Optimized geometries (in Å and deg) for the reactants, transition states (TSs), and products (Pros) of stable cyclic silylene (**3**) with CCl₄ through three reaction pathways, i.e., the one-Cl abstraction (Cl-Abs), the one-CCl₃-group abstraction (CCl₃-Abs), and the insertion reaction (Ins). All were calculated at the B3LYP/6-311G(d) level of theory. The heavy arrows indicate the main components of the transition vector. Hydrogen atoms are omitted for clarity.

profile for this reaction exhibits a maximum. The transition states located for the CCl₃ abstractions by the various stable silylenes are presented in Figures 3–7. Those transition structures are characterized by imaginary frequencies of 441*i*, 453*i*, 474*i*, 476*i*, and 482*i* cm⁻¹ for **1-CCl₃-Abs-TS**, **2-CCl₃-Abs-TS**, **3-CCl₃-Abs-TS**, **4-CCl₃-Abs-TS**, and **5-CCl₃-Abs-TS**, respectively. The normal coordinate corresponding to the imaginary frequency is primarily located at the Cl₃C–Cl bond cleavage, followed by the formation of the Si–CCl₃ bond. As a consequence, the reaction coordinate is fundamentally an asymmetric stretch at the conventional transition state. Additionally, to avoid steric repulsion with the substituents, Si⋯C⋯Cl is slightly bent in these transition states. Moreover, the transition structures show that the newly formed Si–C bond lengths are 2.60 Å (**1-CCl₃-Abs-TS**), 2.52 Å (**2-CCl₃-Abs-TS**), 2.48 Å (**3-CCl₃-Abs-TS**), 2.45 Å (**4-CCl₃-Abs-TS**), and 2.44 Å (**5-CCl₃-Abs-TS**) compared to those in the final radical product (vide infra) of 2.02 Å (**1-CCl₃-Abs-Pro**), 1.98 Å (**2-CCl₃-Abs-Pro**), 1.99 Å (**3-CCl₃-Abs-Pro**), 1.99 Å (**4-CCl₃-Abs-Pro**), and 1.95 Å (**5-CCl₃-Abs-Pro**), respectively. Again, taken together, these features indicate that the transition structures for stable silylene **5** take on a more reactant-like character than that in the stable silylene **2** case. These observations will be related to the predicted energetics below.

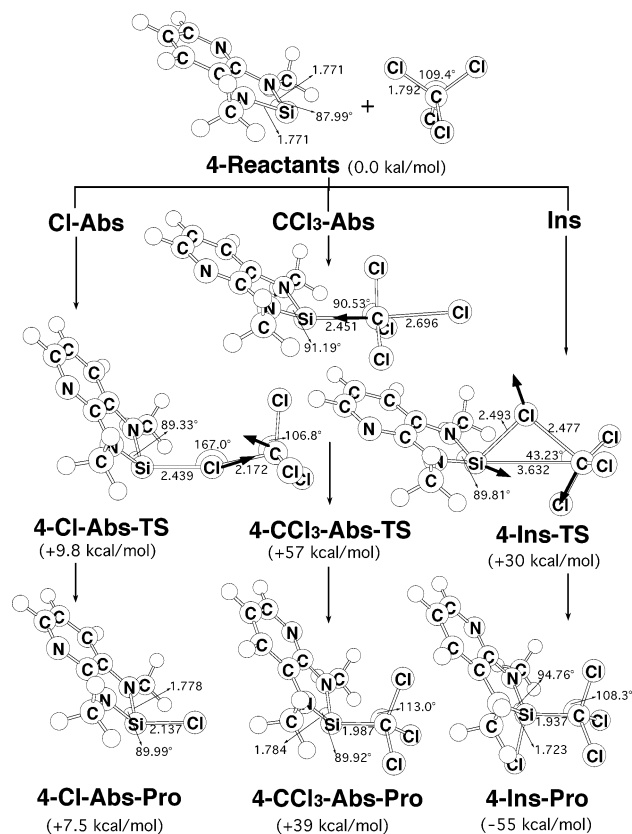


Figure 6. Optimized geometries (in Å and deg) for the reactants, transition states (TSs), and products (Pros) of stable cyclic silylene (**4**) with CCl₄ through three reaction pathways, i.e., the one-Cl abstraction (Cl-Abs), the one-CCl₃-group abstraction (CCl₃-Abs), and the insertion reaction (Ins). All were calculated at the B3LYP/6-311G(d) level of theory. The heavy arrows indicate the main components of the transition vector. Hydrogen atoms are omitted for clarity.

The present calculations predict that the barriers of **1-Cl-Abs-TS**, **2-Cl-Abs-TS**, **3-Cl-Abs-TS**, **4-Cl-Abs-TS**, and **5-Cl-Abs-TS** are 8.9, 8.8, 8.1, 9.8, and 3.6 kcal/mol, respectively. That is, our B3LYP results show that the overall barrier heights are determined to be in the order **5** < **3** < **2** < **1** < **4**. In any event, the above reflects the greater ease of abstracting a chlorine atom with stable silylene **5** over abstraction with stable silylenes **1–4**. Namely, our theoretical findings suggest that the more electropositive the substituents attached to the silicon atom of the silylene, the more facile the abstraction of a chlorine atom from CCl₄ becomes.

The energetics of reactions of the type stable silylene + CCl₄ via path 2 (CCl₃ abstraction) are summarized in Figures 3–7 and in Table 1. The B3LYP calculations indicate that the overall barrier heights with respect to the corresponding reactants are 52 (**1-CCl₃-Abs-TS**), 53 (**2-CCl₃-Abs-TS**), 56 (**3-CCl₃-Abs-TS**), 57 (**1-CCl₃-Abs-TS**), and 47 (**5-CCl₃-Abs-TS**) kcal/mol. Consequently, our theoretical results predict that the process of CCl₃ abstraction with stable silylene **5** is more facile than that with the other stable silylenes **1–4**. That is, the trend is similar to that for the Cl-abstraction reactions described above.

Furthermore, from the computational data discussed above, one can readily see that, for a given stable silylene species, the barrier to Cl abstraction is always smaller than that for CCl₃ abstraction. This may be due to the fact that the site of

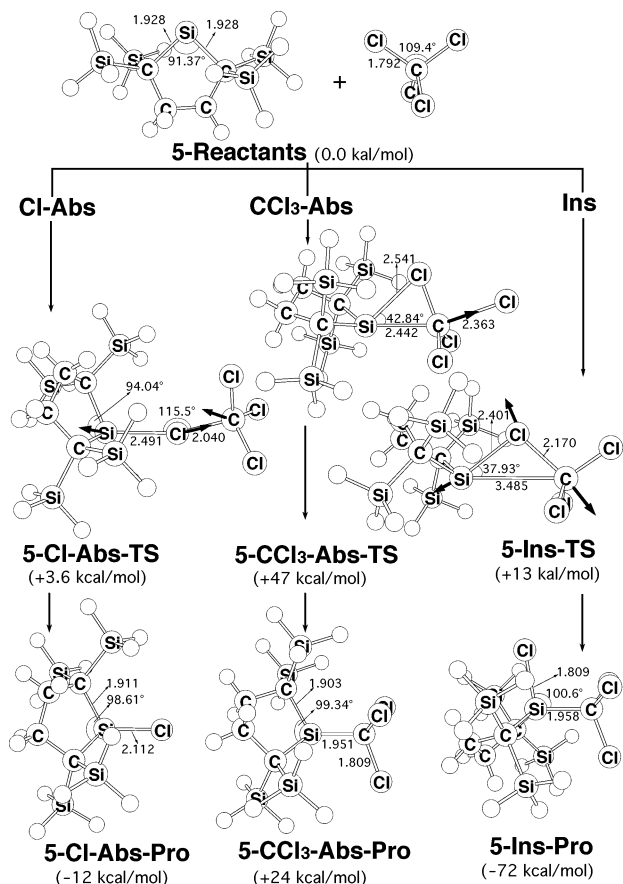


Figure 7. Optimized geometries (in Å and deg) for the reactants, transition states (TSs), and products (Pros) of stable cyclic silylene (5) with CCl₄ through three reaction pathways, i.e., the one-Cl abstraction (Cl-Abs), the one-CCl₃-group abstraction (CCl₃-Abs), and the insertion reaction (Ins). All were calculated at the B3LYP/6-311G(d) level of theory. The heavy arrows indicate the main components of the transition vector. Hydrogen atoms are omitted for clarity.

the stable silylene fragment attacked in the CCl₃-abstraction path is more congested. As a result, it is easier for CCl₄ to approach the stable silylene through the Cl-abstraction path rather than through the CCl₃-abstraction one and, therefore, the former is kinetically favored over the latter. We discuss more about the origin of the barrier heights in a later section.

(3) Abstraction Products. The B3LYP/6-311G(d) geometries of the abstraction products for both reaction pathways (1-Cl-Abs-Pro, 2-Cl-Abs-Pro; 3-Cl-Abs-Pro, 4-Cl-Abs-Pro; 5-Cl-Abs-Pro, 1-CCl₃-Abs-Pro; 2-CCl₃-Abs-Pro, 3-CCl₃-Abs-Pro; 4-CCl₃-Abs-Pro, and 5-CCl₃-Abs-Pro) are displayed in Figures 3–7, respectively. To simplify comparisons and to emphasize the trends, the calculated reaction enthalpies for abstraction are also collected in Table 1. Unfortunately, experimental structures for these abstraction products are not yet known.

As discussed previously, a stable silylene (such as 5) with two carbon atoms bonded to silicon and with no resonance structure reaches the transition state relatively early, whereas a stable silylene (such as 1–4) with two nitrogen atoms bonded to silicon and containing a resonance structure arrives relatively late. The former is therefore predicted to undergo a more exothermic abstraction, which is borne out by our theoretical calculations. For example, the order of enthalpy

follows a trend similar to that of the activation energy: 4-Cl-Abs-Pro (+7.5 kcal/mol) > 3-Cl-Abs-Pro (+7.2 kcal/mol) > 2-Cl-Abs-Pro (+5.7 kcal/mol) > 1-Cl-Abs-Pro (+4.8 kcal/mol) > 5-Cl-Abs-Pro (-12 kcal/mol) and 4-CCl₃-Abs-Pro (+39 kcal/mol) ≈ 3-CCl₃-Abs-Pro (+39 kcal/mol) > 2-CCl₃-Abs-Pro (+37 kcal/mol) > 1-CCl₃-Abs-Pro (+36 kcal/mol) > 5-CCl₃-Abs-Pro (+24 kcal/mol). Note that the energies of the CCl₃-abstraction products are all above those of their corresponding reactants. This strongly indicates that CCl₃-abstraction reactions with stable silylenes are energetically unfavorable and would be endothermic. That is to say, our computational results suggest that the abstraction products (stable silylene)CCl₃• are not produced from a CCl₃ group transfer reaction, silylene + CCl₄ → (stable silylene)-CCl₃• + Cl•, but possibly exist if these radicals are produced through other reaction paths.

In brief, the present calculations suggest the following about the radical mechanism for the stable silylene + CCl₄ reaction: (1) The Cl-abstraction pathway is more favorable than the CCl₃-abstraction pathway from both kinetic as well as thermodynamic considerations. (2) One of the reasons for the lower activation energy of path 1 (Cl abstraction) is presumably less repulsion between the chlorine atom and the substituents of the stable silylene. The site of the stable silylene moiety attacked in path 2 (CCl₃ abstraction) is more congested. As a result, it is easier for CCl₄ to approach the silicon atom of the stable silylene through Cl abstraction rather than through CCl₃ abstraction. (3) Our model calculations demonstrate that a silylene containing a silicon atom bonded to two carbon atoms and containing no resonance structure reaches an early transition state. This, in turn, results in a lower barrier to abstraction and an increased exothermicity.

(4) Transition States for Insertion Reactions. We next consider the insertion reaction of the stable silylenes with CCl₄. The fully optimized B3LYP/6-311G(d) geometries of the transition states and products are shown in Figures 3–7. Moreover, their relative energies, calculated at the B3LYP/6-311G(d) level, are given in Table 1.

The transition-state geometries for the insertions of stable silylenes 1–5 into the C–Cl bond of CCl₄ are depicted in Figures 3–7. All of these transition states possess one imaginary frequency and are true first-order saddle points. The calculated imaginary frequencies are 206*i*, 245*i*, 217*i*, 255*i*, and 244*i* cm⁻¹ for 1-Ins-TS, 2-Ins-TS, 3-Ins-TS, 4-Ins-TS, and 5-Ins-TS, respectively. The arrows in the figures illustrate the direction in which the atoms move in the normal coordinate corresponding to the imaginary frequency. In these transition states, the chlorine atom is positioned under the Si–C bond, forming a three-membered ring. The DFT calculations suggest that the barrier height for Si–Cl bond insertion decreases in the order 1-Ins-TS (31 kcal/mol) ≈ 3-Ins-TS (31 kcal/mol) > 4-Ins-TS (30 kcal/mol) > 2-Ins-TS (28 kcal/mol) > 5-Ins-TS (13 kcal/mol). Also, note that at these transition states the breaking C–Cl bond is stretched by 43% (1-Ins-TS), 36% (2-Ins-TS), 29% (3-Ins-TS), 38% (4-Ins-TS), and 21% (5-Ins-TS), respectively, relative to the equilibrium C–Cl distance (1.792

Å) in CCl₄. Accordingly, the barrier is encountered earlier in the reaction of stable silylene **5** than for the other stable silylene species (**1–4**). We see the energetics reflecting these facts below.

(5) Insertion Products. The equilibrium geometries for the insertion products (**1-Ins-Pro**, **2-Ins-Pro**, **3-Ins-Pro**, **4-Ins-Pro**, and **5-Ins-Pro**) are presented in Figures 3–7, respectively. The reaction enthalpies at the B3LYP level of theory are outlined in Table 1. The theoretical results, given in Figures 3–7, show that all of the insertion products adopt a tetracoordinate conformation at the silicon center. Unfortunately, experimental structures for these insertion products are not known.

Furthermore, it is apparent that all of the silylene insertions are thermodynamically exothermic. Moreover, as shown in Table 1, the main difference between the first four stable silylenes (**1–4**) and stable silylene **5** is that the reaction of the latter is more exothermic and its activation barrier lower. Again, this result is consistent with the prediction that the activation barrier should be correlated with the exothermicity.¹⁹ As demonstrated in Table 1, the order of enthalpy follows a trend similar to that of the activation energy: **2-Ins-Pro** (–63 kcal/mol) > **1-Ins-Pro** (–51 kcal/mol) > **3-Ins-Pro** (–55 kcal/mol) ≈ **4-Ins-Pro** (–55 kcal/mol) > **5-Ins-Pro** (–72 kcal/mol). Combining the theoretical data, it is clear, from both a kinetic and a thermodynamic viewpoint, that the insertion reaction of stable silylene **5** is much more favorable than those of the other stable silylene species (**1–4**).

In short, the trends in the energetics of these five stable silylene systems are especially interesting. First, our theoretical findings indicate that for stable silylene insertions there is a very clear trend toward lower activation barriers and more exothermic interactions on going from silylene **1** to silylene **5**. Second, the insertion reaction is more exothermic, but the reaction barrier is lower for the abstraction reactions.

IV. Overview of Abstraction and Insertion Reactions of Stable Silylenes

From our study of the mechanisms of the reactions of stable silylenes (**1–5**) with CCl₄, the major conclusions that can be drawn are as follows:

(1) In the competition between abstraction and insertion reactions with CCl₄, abstraction predominates for any given stable silylene species. Nevertheless, the insertion reaction is more exothermic, but its barrier height is greater.

(2) On the other hand, in the competition between chlorine (Cl) and CCl₃ abstraction, the CCl₃ abstraction has the highest energy requirement and the largest endothermicity. As a result, this makes it the least energetically favorable abstraction pathway. Cl abstraction will therefore be the first step in the initial reaction of a stable silylene and carbon tetrachloride, and Cl-abstraction products will dominate.

(3) The theoretical results suggest that a singlet stable silylene inserts in a concerted manner via a three-center-

type transition state and that the stereochemistry at the silicon center is preserved.

(4) For a given haloalkane (carbon tetrachloride in the present work), the stability of a silylene (such as **1–4**) is mainly due to a combination of the electron-donating properties of the electron-rich π system and the σ -electron-withdrawal effect of the electronegative nitrogen atoms adjacent to the silylene center. However, this is not the case for stable silylene **5**. Accordingly, silylene **5** may be relatively susceptible toward the reactions with haloalkanes, especially in comparison with the other stable silylenes (**1–4**). This means that stable silylene **5** can undergo either abstraction or insertion reactions with haloalkanes.

V. Configuration Mixing Model

In this section, an intriguing model for interpreting the relative reactivity of the reactant species is provided by the so-called configuration mixing (CM) model, which is based on the work of Pross and Shaik.^{20,21} According to the conclusions of this model, the energy barriers governing processes as well as the reaction enthalpies should be proportional to the energy gaps for both stable silylene and carbon tetrahalide, that is, proportional to ΔE_{st} ($=E_{\text{triplet}} - E_{\text{singlet}}$ for stable silylene) + $\Delta E_{\sigma\sigma^*}$ ($=E_{\text{triplet}} - E_{\text{singlet}}$ for CCl₄). We thus conclude that both the order of the singlet and triplet states and their energy separation are responsible for the existence and the height of the energy barriers.^{20,21} Bearing this CM model in mind, we explain the origin of the previously observed trends in the following discussion:

(1) *Why does the reactivity of stable silylene abstraction and insertion reactions increase in the order 2 < 3 < 4 < 1 < 5?*

The reason for this can be traced to the singlet–triplet energy gap of the stable silylene. That is to say, the smaller ΔE_{st} for the stable silylene, the lower the barrier height and the larger the exothermicity and, in turn, the faster the chemical reaction. As one can see in Table 1, our B3LYP results suggest a decreasing trend in ΔE_{st} of **2** (68 kcal/mol) > **3** (60 kcal/mol) > **4** (59 kcal/mol) > **1** (53 kcal/mol) > **5** (34 kcal/mol). This correlates well with the trend in both barrier height and exothermicity, as demonstrated in the previous section. Namely, our theoretical findings are in good agreement with the CM model.

VI. Conclusion

In the present work, we have studied the reaction mechanisms of stable silylene (**1–5**) abstractions and insertions with carbon tetrachloride using DFT. It should be pointed out that this study has provided the first theoretical demon-

(19) Chen, C.-H.; Su, M. D. *Chem.—Eur. J.* **2007**, *13*, 6932.

(20) For details, see: (a) Shaik, S.; Schlegel, H. B.; Wolfe, S. In *Theoretical Aspects of Physical Organic Chemistry*; John Wiley & Sons Inc.: New York, 1992. (b) Pross, A. In *Theoretical and Physical Principles of Organic Reactivity*; John Wiley & Sons Inc.: New York, 1995. (c) Shaik, S. *Prog. Phys. Org. Chem.* **1985**, *15*, 197. (d) Su, M.-D. *Chem.—Eur. J.* **2004**, *10*, 5877.

(21) (a) For the first paper that originated the CM model, see: Shaik, S. *J. Am. Chem. Soc.* **1981**, *103*, 3692. (b) For the most updated review of the CM model, see: Shaik, S.; Shurki, A. *Angew. Chem., Int. Ed.* **1999**, *38*, 586.

stration about the reaction trajectory and theoretical estimation of the activation energy and reaction enthalpy for these processes. Moreover, we have demonstrated that the computational results can be rationalized using a simple CM model. Thus, not only have we given an explanation of the present theoretical observations, but also we have made predictions for the reaction of stable silylenes with haloalkanes.

The theoretical results suggest that the stability of a silylene is mainly attributed to the electron-donating properties of the electron-rich π system as well as to the σ -electron-withdrawal effect of the electronegative nitrogen atoms adjacent to the silylene center, which in turn leads to an increase in the singlet–triplet energy gap. This results in a greater ΔE_{st} , a larger activation barrier, and a smaller reaction enthalpy and stabilizes the silylene itself. Also, our model calculations indicate that, in the competition between abstraction and insertion reactions with CCl₄, stable silylenes

prefer to undergo one-Cl abstraction rather than CCl₃ abstraction or insertion reactions. Unfortunately, as we have mentioned earlier, because of a lack of experimental and theoretical data on such abstraction and insertion reactions, our conclusions above may be considered as predictions for future investigations.

We thus encourage experimentalists to carry out further experiments to confirm our predictions.

Acknowledgment. We are very grateful to the National Center for High-Performance Computing of Taiwan for generous amounts of computing time. We also thank the National Science Council of Taiwan for their financial support.

Supporting Information Available: Atomic numbers and coordinates for various compounds given in the text. This material is available free of charge via the Internet at <http://pubs.acs.org>.

IC7012446